Coulomb-Born calculation of the triple-differential cross section for inner-shell electron-impact ionization of carbon

J. Botero* and J. H. Macek
University of Tennessee, Knoxville, Tennessee 37996-1200
and Oak Ridge National Laboratory, Oak Ridge, Tennessee 37831-6373
(Received 5 August 1991)

A Coulomb-Born approximation is used to compute the triple-differential cross section for electron-impact inner-shell ($1s$) ionization of carbon. We employ a perturbation series that allows the use of Coulomb waves with arbitrary Z_{eff} for the incoming, scattered, and ejected electrons. Most of the features of the triple-differential cross section observed experimentally are reproduced, even though these wave functions are distorted by an effective Coulomb potential and therefore do not satisfy the plane-wave boundary conditions at infinity. In order to explain some features that appear in the cross section, and in order to probe the validity of a dipole approximation, we make a multipole expansion of the transition matrix and show that the amplitudes of the multipole components are similar to those obtained in the Born approximation, while the relative phases of the multipoles differ greatly.

PACS number(s): 34.80.Dp

I. INTRODUCTION

The study of $(e,2e)$ reactions, e.g., single-step electron-impact ionization of atoms, has gained much attention, both experimentally and theoretically, during the past two decades, especially after the experimental work of Ehrhardt *et al.* [1]. The triple-differential cross section (TDCS) of these reactions [even though it is actually a fivefold-differential cross section, we will call it triple-differential cross section in order to agree with the current $(e,2e)$ literature] is an explicit function of all the collision parameters: the energy of the incoming electron, the energy and direction of the scattered electron, and the energy and direction of the ejected electron. Therefore, the information gained in its study is extremely useful to the understanding of fundamental collision dynamics [2]. Several theoretical studies have been devoted to $(e,2e)$ reactions in hydrogen and helium [2–8], while very few have studied $(e,2e)$ reactions from inner shells of heavier atoms [9].

Recent measurements of the TDCS of electron-impact ionization of inner shells of carbon [9], neon [10], and argon [10–12] have shown that the plane-wave Born approximation (PBA) fails to reproduce most of the structural parameters of the TDCS [1], such as the ratio of the binary and recoil peaks and their angular position. This is not surprising, since it is well known that the PBA is only appropriate for inner shells when the parameter $a=2\pi Z_{\text{eff}}/v$, where Z_{eff} is the effective charge of the target and v is the velocity of the projectile, is much less than unity. For the ionization of inner shells of carbon, this would require an initial energy of the order of 20 keV, while experiments are done at energies of the order of 1 keV. Accordingly, a distorted-wave approximation must be used.

It is generally considered that, using standard perturbation expansions, the decrease of the Coulomb field with distance must be taken into account [13–15] in the unperturbed wave functions; otherwise, a divergent phase is involved in the calculation of the scattering amplitude [15,16]. Here we show that, by using a perturbation series introduced earlier [8], one may simultaneously employ well-defined expressions for transition amplitudes yet obtain first-order expressions where the wave functions are not constrained by the slow decrease of the potential at large distances. This expansion allows the use of Coulomb waves with arbitrary Z_{eff} for the incoming and scattered electrons, even though they do not satisfy correct asymptotic conditions, and therefore it extends the use of the Coulomb-Born approximation (CBA) to the scattering of charged particles from neutral atoms.

We compute the TDCS for electron-impact ionization of inner shells ($1s$) of Carbon using this perturbation theory and find that many features of the TDCS, such as the ratio between the binary and recoil peaks and their angular position, are reproduced by the theory. We analyze our results by a multipole expansion of the transition matrix and compare individual multipoles with results from PBA and find that, at the energies where the experiments were done [9], the contribution from the quadrupole term is still appreciable and therefore a dipole approximation is not valid. We also find that the amplitude of the different multipoles are very similar in CBA and PBA, while their relative phases are different.

This paper is organized as follows: in Sec. II we review briefly the standard perturbation expansion for Coulomb functions and the difficulties it presents, and review two "nontraditional" solutions presented earlier [8,16] to overcome these difficulties; in Sec. III we apply the perturbation expansion to the transition matrix; in Sec. IV we derive the expressions used to compute the TDCS; in Sec. V we present the results for carbon and analyze them based on a multipole expansion of the transition matrix both in CBA and PBA; and Sec. VI consists of a summary and conclusions. Details of the evaluation of integrals and derivatives, as well as an analytical proof of the orthogonality of the dipole components and the

derivation of the multipole expansion in PBA, are given in Appendixes A–C. Atomic units are used throughout.

II. PERTURBATION EXPANSION FOR COULOMB FUNCTIONS

Consider the Hamiltonian for an electron in a Coulomb field

$$H=K_0+\left[-\frac{Z}{r}\right], \tag{1}$$

$$H(\lambda)=K_0+\lambda U , \tag{2}$$

where we are treating $U=-Z/r$ as a perturbation and λ has been introduced to order the perturbation series. The eigenfunctions of $H(\lambda)$ are Coulomb functions $\psi_k^+(\mathbf{r},\lambda)$, which are now functions of the perturbation parameter λ:

$$\psi_{\mathbf{k}}^+(\mathbf{r},\lambda)=(2\pi)^{-3/2}e^{-\pi i a/2}\Gamma(1-a) \times e^{i\mathbf{k}\cdot\mathbf{r}}{}_1F_1(a,1;i(kr-\mathbf{k}\cdot\mathbf{r})) \tag{3}$$

$$=N_k^{(+)}e^{i\mathbf{k}\cdot\mathbf{r}}{}_1F_1(a,1;i(kr-\mathbf{k}\cdot\mathbf{r})) , \tag{4}$$

where $a=i\nu=i\lambda Z/k$.

Standard perturbation theories expand the eigenfunctions of H, $\psi_{\mathbf{k}}^+(\mathbf{r})$, in powers of λ:

$$\psi_{\mathbf{k}}^+(\mathbf{r})=\sum_n \lambda^n\psi_{\mathbf{k}}^{(n)+}(\mathbf{r}) , \tag{5}$$

and compute the coefficients of λ^n directly from the perturbation equations

$$(K_0-E)\psi_{\mathbf{k}}^{(0)+}=0 , \tag{6}$$

$$(K_0-E)\psi_{\mathbf{k}}^{(1)+}=-U\psi_{\mathbf{k}}^{(0)+} , \tag{7}$$

$$(K_0-E)\psi_{\mathbf{k}}^{(n)+}=-U\psi_{\mathbf{k}}^{(n-1)+} . \tag{8}$$

To this end, Eq. (7) is integrated using the standard Green-function approach:

$$\psi_{\mathbf{k}}^{(1)+}=(E+i\eta-H_0)^{-1}U\phi_{\mathbf{k}} , \tag{9}$$

where $\phi_{\mathbf{k}}(\mathbf{r})=\psi_{\mathbf{k}}^{(0)+}$ is a plane wave.

The right-hand side is evaluated by writing the Green function in the momentum representation, so that the above equation becomes

$$\psi_{\mathbf{k}}^{(1)+}=\frac{-8\pi Z}{(2\pi)^{3/2}}\int\frac{\exp(i\mathbf{p}\cdot\mathbf{r})}{k^2+2i\eta-p^2}\frac{1}{|\mathbf{p}-\mathbf{k}|^2}d\mathbf{p} . \tag{10}$$

This expression is a special case of the two-denominator integral which can be evaluated using Feynman integration to obtain [13]

$$\psi_{\mathbf{k}}^{(1)+}=Z\phi_{\mathbf{k}}(\mathbf{r})\int_0^1 dx\frac{\exp\{[-i\mathbf{k}\cdot\mathbf{r}x+i\sqrt{(kx+i\eta/k)^2+(\eta/k)^2}]r\}}{-i\sqrt{(kx+i\eta/k)^2+(\eta/k)^2}} . \tag{11}$$

This integral diverges in the limit $\eta\to 0$. For nonzero, but sufficiently small, η we may write

$$\psi_{\mathbf{k}}^{(1)+}=\frac{\mu Z}{-ik}\phi_{\mathbf{k}}(\mathbf{r})\left[\int_0^1 dx\frac{\exp[i(kr-\mathbf{k}\cdot\mathbf{r})x-1]}{x}+\int_0^1\frac{dx}{\sqrt{x^2+2i\eta x/k^2}}\right] . \tag{12}$$

The integral in the first term in large parentheses on the right-hand side of Eq. (12) is readily evaluated in terms of the exponential integral $\mathrm{Ei}[i(kr-\mathbf{k}\cdot\mathbf{r})]$. The second integral is elementary and we have, in the limit of small η,

$$\psi_{\mathbf{k}}^{(1)+}=i\nu\phi_{\mathbf{k}}(\mathbf{r})\{\mathrm{Ei}[i(kr-\mathbf{k}\cdot\mathbf{r})] -\ln[i(kr-\mathbf{k}\cdot\mathbf{r})]-\ln(i\eta/2k^2)\} . \tag{13}$$

This expression diverges logarithmically as $\eta\to 0$ and therefore it cannot represent a solution of Eq. (7).

Here we review briefly two different approaches that have been presented to overcome this difficulty. One is based on the definition of the on-shell scattering states of Roberts [17],

$$\psi_{\mathbf{k}}^+=\lim_{z\to E_k}a(z,E)\psi_{\mathbf{k},z}^+ , \tag{14}$$

where $z=E+i\eta$, E_k is the eigenvalue of K_0, $\psi_{\mathbf{k},z}^+$ is the off-shell scattering state, and $a(z,E_k)$ is given by [16]

$$a(z,E_k)^{-1}=[(E_k-z)/4E_k]^{i\nu}e^{i\varphi(i\nu)}\Gamma'(1+i\nu) , \tag{15}$$

where $\varphi(i\nu)$ is a phase factor, which in Ref. 16 was set equal to $\pi i\nu/2$, and where we have set $E_k>E$, e.g., $\eta\to 0+$.

The expansion of $\psi_{\mathbf{k}}^+$ in powers of λ now may be written as

$$\psi_{\mathbf{k}}^+(\mathbf{r})=\lim_{z\to E_k}\left[\sum_{s=0}^{\infty}a^{(s)}(z,E_k)\lambda^s\right]\sum_{m=0}^{\infty}\lambda^m\psi_{\mathbf{k},z}^{(m)+}(\mathbf{r}) =\lim_{z\to E_k}\sum_{n=0}^{\infty}\lambda^n\left[\sum_{s=0}^{\infty}a^{(s)}(z,E_k)\psi_{\mathbf{k},z}^{(n-s)+}(\mathbf{r})\right] , \tag{16}$$

so that the coefficients of λ^n are

$$\psi_{\mathbf{k}}^{(n)+}(\mathbf{r})=\lim_{z\to E_k}\sum_{s=0}^{\infty}a^{(s)}(z,E_k)\psi_{\mathbf{k},z}^{(n-s)+}(\mathbf{r}) , \tag{17}$$

and the first-order term is then

$$\psi_{\mathbf{k}}^{(1)+}(\mathbf{r})=\lim_{z\to E_k}[a^{(1)}\psi_{\mathbf{k},z}^{(0)+}+a^{(0)}(z,E_k)(z-E_k)^{-1}\psi_{\mathbf{k},z}^{(0)+}] . \tag{18}$$

Since $a^{(0)}=1$ and $a^{(1)}$ contains a logarithmic divergence [16] of the form $(i\nu\ln\eta)$ which cancels the divergence in the second term, this expression for $\psi_k^{(1)+}$ is well defined

and gives convergent functions which behave asymptotically as

$$\psi_{\mathbf{k}}^{(1)+} \rightarrow [-i\nu \ln(kr - \mathbf{k}\cdot\mathbf{r}) + (\text{constant terms})]\psi_{\mathbf{k}}^{(0)+} , \quad (19)$$

in agreement with the expansion of the asymptotic form of Coulomb wave functions.

An alternative way [8] of obtaining the coefficients of λ^n is by recognizing the expansion of $\psi_{\mathbf{k}}^{+}$ [Eq. (5)] as a Taylor series expansion around the point $\lambda=0$, and evaluate $\psi_{\mathbf{k}}^{(n)+}(\mathbf{r})$ directly from the known Coulomb functions, now functions of λ through the parameter $a = i\lambda Z/K_i$, that is,

$$\psi_{\mathbf{k}}^{(n)+}(\mathbf{r}) = \frac{1}{n!}\frac{\partial^n}{\partial\lambda^n}\psi_k^{+}(\mathbf{r},\lambda)\bigg|_{\lambda=0} , \quad (20)$$

which gives perfectly well-defined functions. They are easily seen to satisfy Eqs. (6)–(8), but are not given by the usual representation of Eq. (9). Rather they are given by Eq. (17) or, equivalently, by Eq. (20). We prefer Eq. (20) for practical calculations.

III. PERTURBATION THEORY WITH ARBITRARY BOUNDARY CONDITIONS FOR ELECTRON SCATTERING

In this section we apply the perturbation series introduced in Ref. [8] and presented in the last part of the previous section to electron scattering from atoms. Standard perturbation theories may be used in two different cases. First, when the Hamiltonian of a system is such that a part of it is small compared to the rest, we introduce a strength parameter λ to multiply the small part of the Hamiltonian and then expand the wave function in powers of this parameter. Second, when eigenfunctions of an approximate Hamiltonian H_{approx}, possibly valid at those regions of space where the interactions occur, are known, we add and subtract this approximate Hamiltonian to the exact one H, and introduce the strength parameter λ to multiply the difference $H - H_{\text{approx}}$, and then expand the wave function in powers of this parameter. In both cases we get the exact Hamiltonian H when $\lambda=1$ and the approximate Hamiltonian H_{approx} when $\lambda=0$. The objective is therefore to interpolate wave functions and T matrices between these points.

The Hamiltonian for a system of an $(N-1)$-electron atom plus an incoming (or outgoing) electron may be written as

$$H = H_0 + V_0 + V_{\text{int}} , \quad (21)$$

where H_0 is the kinetic-energy operator for N electrons, V_0 is the potential of the $(N-1)$ target electrons in the field of the nucleus of charge Z,

$$V_0 = \sum_{i=1}^{N-1} -\frac{Z}{r_i} + \sum_{i\neq j}\frac{1}{r_{ij}} , \quad (22)$$

V_{int} is the interaction potential of electron N with the target ion

$$V_{\text{int}} = -\frac{Z}{r_N} + \sum_{i-1}^{N-1}\frac{1}{r_{Ni}} , \quad (23)$$

r_N is the coordinate of electron N and $r_{ij} = 1/|r_i - r_j|$. In the limit $r_N \rightarrow \infty$, we have

$$V_{\text{int}} \rightarrow (-Z + N - 1)/r_N = -Q/r_N , \quad (24)$$

where $Q = Z - N + 1$ is the net charge of the ion in the initial state.

We define an effective potential for the electron N as $V_{\text{eff}} = -Z_{\text{eff}}/r_N$ with Z_{eff} arbitrary, and a short-range interaction potential $V'_{\text{int}} = V_{\text{int}} + Q/r_N$, such that $V'_{\text{int}} \rightarrow 0$ as $r_N \rightarrow \infty$. We then write the Hamiltonian as

$$H = H_0 + V_0 + V_{\text{eff}} + (V_{\text{int}} - V_{\text{eff}}) , \quad (25)$$

and treat $(V_{int} - V_{\text{eff}})$ as a perturbation:

$$\begin{aligned} H(\lambda) &= H_0 + V_0 + V_{\text{eff}} + \lambda(V_{\text{int}} - V_{\text{eff}}) \\ &= H_0 + V_0 + V_{\text{eff}} + \lambda U_Q + \lambda V'_{\text{int}} , \end{aligned} \quad (26)$$

where $U_Q = (Z_{\text{eff}} - Q)/r_N$. Clearly, when $\lambda=1$ we recover the exact Hamiltonian, and when $\lambda=0$ we obtain the "initial" Hamiltonian of the $(N-1)$ electron target ion plus electron N in the field of a nucleus of charge Z_{eff}. The Hamiltonian $H(\lambda)$ may be written as

$$H(\lambda) = \mathcal{H}_T + \mathcal{H}(\lambda) + \lambda V'_{\text{int}} , \quad (27)$$

where

$$\mathcal{H}_T = H_0 - K_0 + V_0 \quad (28)$$

is the Hamiltonian for the $(N-1)$ target electrons, and

$$\mathcal{H}(\lambda) = K_0 + V_{\text{eff}} + \lambda U_Q \quad (29)$$

is the Hamiltonian for electron N with kinetic energy K_0. The initial and final states are products of the target eigenstates Φ_i and Φ_f and the Coulomb wave functions $\psi^{\pm}_{\mathbf{K}_{i/f}}(\mathbf{r}_N,\lambda)$, which are now functions of the perturbation parameter λ. Our perturbation series is obtained by expanding the T matrix in powers of λ. This means that the wave functions $\psi^{\pm}_{\mathbf{K}_{i/f}}(\mathbf{r}_N,\lambda)$ must also be expanded in powers of λ, but, since $V_{\text{eff}} - \lambda U_Q$ is a Coulomb potential, the usual Green-function representation of this expansion is not valid. The expansion, however, is readily carried out directly. The desired functions are

$$\begin{aligned} \psi^{(+)}_{\mathbf{K}_i}(\mathbf{r},\lambda) &= (2\pi)^{-3/2} e^{-\pi i a/2}\Gamma(1-a) \\ &\quad \times e^{i\mathbf{K}_i\cdot\mathbf{r}}\,{}_1F_1(a,1;i(K_i r - \mathbf{K}_i\cdot\mathbf{r})) \\ &= N^{(+)}_{K_i} e^{i\mathbf{K}_i\cdot\mathbf{r}}\,{}_1F_1(a,1;i(K_i r - \mathbf{K}_i\cdot\mathbf{r})) \end{aligned} \quad (30)$$

and

$$\begin{aligned} \psi^{(-)}_{\mathbf{K}_i}(\mathbf{r},\lambda) &= (2\pi)^{-3/2} e^{-\pi i b/2}\Gamma(1+b) \\ &\quad \times e^{i\mathbf{K}_f\cdot\mathbf{r}}\,{}_1F_1(-b,1;-i(K_f r - \mathbf{K}_f\cdot\mathbf{r})) \\ &= N^{(+)}_{K_f} e^{i\mathbf{K}_f\cdot\mathbf{r}}\,{}_1F_1(-b,1;-i(K_f r + \mathbf{K}_f\cdot\mathbf{r})) , \end{aligned} \quad (31)$$

where

$$a = i[Z_{\text{eff}} - \lambda(Z_{\text{eff}} - Q)]/K_i \quad (32)$$

and

$$b = i[Z_{\text{eff}} - \lambda(Z_{\text{eff}} - Q)]/K_f \ . \tag{33}$$

Note that, when $\lambda=0$, the functions $\psi^{\pm}_{\mathbf{K}_{i/f}}(\mathbf{r}_N,\lambda)$ are Coulomb functions with an effective charge Z_{eff}.

The transition matrix element is then

$$T_{fi}(\lambda) = \langle \psi^{-}_{\mathbf{K}_f}(\lambda)\Phi_f | \lambda V'_{\text{int}} + \lambda^2 V'_{\text{int}} G^{+}(\lambda) V'_{\text{int}} | \psi^{+}_{\mathbf{K}_i}(\lambda)\Phi_i \rangle \ , \tag{34}$$

where $G^{+}(\lambda)=[E+i\eta-H(\lambda)]^{-1}$ is the Green function of the Hamiltonian $H(\lambda)$. Note that this expression is well defined for all λ, in contrast to expressions [18] that use $V'_{\text{int}} \rightarrow V_{\text{int}} - V_{\text{eff}}$ and Coulomb functions $\psi^{\pm}_{\mathbf{K}_{i/f}}(\mathbf{r})$ which are independent of λ.

We now expand the T matrix in power series of λ:

$$T_{fi}(\lambda) = \sum_n \lambda^n T^{(n)}_{fi} \ , \tag{35}$$

and evaluate the coefficients $T^{(n)}_{fi}$ by

$$T^{(n)}_{fi} = \frac{1}{n!} \frac{\partial^n T_{fi}(\lambda)}{\partial \lambda^n} \bigg|_{\lambda=0} \ . \tag{36}$$

The lowest-order term is, as usual, $T^{(0)}_{fi}=0$, and the first-order term is given by

$$\begin{aligned} T^{(1)}_{fi} &= \langle \psi^{-}_{\mathbf{k}'}(\mathbf{r},0)\Phi_f(\mathbf{r}') | V'_{\text{int}} | \psi^{+}_{\mathbf{k}}(\mathbf{r},0)\Phi_i(\mathbf{r}') \rangle \\ &= \langle \psi^{-}_{\mathbf{k}'}(\mathbf{r},0)\Phi_f(\mathbf{r}') | V_{\text{int}} | \psi^{+}_{\mathbf{k}}(\mathbf{r},0)\Phi_i(\mathbf{r}') \rangle \ , \end{aligned} \tag{37}$$

where the orthogonality of initial and final target eigenstates has been used to eliminate Q/r_N. This is just the desired expression since the distorted waves are Coulomb waves in an attractive potential with the arbitrary strength parameter Z_{eff}.

The second-order term is not the conventional result of distorted-wave theory, rather, we have

$$\begin{aligned} T^{(2)}_{fi} = \frac{\partial}{\partial\lambda} \langle \psi^{-}_{\mathbf{k}'}(\lambda)\Phi_f | V_{\text{int}} | \psi^{+}_{\mathbf{k}}(\lambda)\Phi_i \rangle |_{\lambda=0} \\ + \langle \psi^{-}_{\mathbf{k}'}(0)\Phi_f | V'_{\text{int}} \ G^{+}(0) V'_{\text{int}} | \psi^{+}_{\mathbf{k}}(0)\Phi_i \rangle \ . \end{aligned} \tag{38}$$

Since the derivatives of the Coulomb functions are well defined, as noted above, and since $V'_{\text{int}} \rightarrow 0$ as $r_N \rightarrow \infty$ faster than $1/r_N$, it is easily seen that $T^{(2)}_{fi}$ is finite and well defined. Alternatively, if the standard Green's-function solution of the perturbation equation, namely,

$$\psi^{(n)\pm}_{\mathbf{k}} \stackrel{?}{=} (E+i\eta-K_0-V_{\text{eff}})^{-1} U_Q \psi^{(n-1)\pm}_{\mathbf{k}} \tag{39}$$

is used to compute the derivative of the Coulomb functions with respect to the parameter λ, one obtains the usual expression

$$T^{(2)}_{fi} \stackrel{?}{=} \langle \psi^{-}_{\mathbf{k}'}(0)\Phi_f | (V_{\text{int}} - V_{\text{eff}}) G^{+}(0) (V_{\text{int}} - V_{\text{eff}}) | \psi^{+}_{\mathbf{k}}(0)\Phi_i \rangle , \tag{40}$$

which diverges unless $Z_{\text{eff}}=Q=0$ for neutral atoms. In contrast, our perturbation series allows complete freedom in choosing Z_{eff} and thereby extends the Coulomb-Born approximation to scattering from neutral systems, such as atomic carbon.

IV. TRIPLE-DIFFERENTIAL CROSS SECTION

In the present work we apply the perturbation expansion presented above to calculate the TDCS for electron-impact ionization of inner shells of carbon. To this end we approximate the interaction potential by a two-particle potential, namely, $V_{\text{int}}=1/|\mathbf{r}-\mathbf{r}'|$, where $\mathbf{r}$ and $\mathbf{r}'$ are the coordinates of the incoming (or scattered) electron and the atomic (or ejected) electron, respectively. The transition matrix element is therefore given to first order in λ by

$$T_{fi} = \left\langle \psi^{(-)}_{\mathbf{K}_f}(\mathbf{r}) \psi^{(-)}_{\mathbf{k}}(\mathbf{r}') \left| \frac{1}{|\mathbf{r}-\mathbf{r}'|} \right| \varphi_i(\mathbf{r}') \psi^{(+)}_{\mathbf{K}_i}(\mathbf{r}) \right\rangle \ , \tag{41}$$

where the initial target eigenstate is approximated by a hydrogenic function for the active $1s$ electron $\varphi_i(r')=Z_T^{3/2}\pi^{-1/2}e^{-Z_T r'}$, with Z_T equal to the screened charge of the target chosen such that it gives the binding energy of the $1s$ electron, and the final target wave function is approximated by a Coulomb wave with the same effective charge. The initial and final eigenstates of the projectile are, as noted in previous sections, Coulomb waves with an effective charge Z_{eff}. Note that this approximation for $(e,2e)$ reactions amounts to treating electron-electron collisions in the presence of an external field, the external field being a Coulomb field of strength Z_{eff}. Because of the passive atomic $1s$ electron, Z_T and Z_{eff}, in general, differ, but we take them to be equal. We compute the direct T-matrix element $T^{d}_{fi}(\mathbf{K}_i,\mathbf{K}_f,\mathbf{k})$ from Eq. (41) and use the exact relation

$$T^{\text{ex}}_{fi}(\mathbf{K}_i,\mathbf{K}_f,k) = T_{fi}(\mathbf{K}_i,\mathbf{k},\mathbf{K}_f) \ , \tag{42}$$

valid for the exact T matrix, to compute the exchange amplitude.

The TDCS corresponding to ejection of an atomic $1s$ electron with momentum $\mathbf{k}$ (see Fig. 1) into the solid angle $d\Omega_k$, and to scattering of the incident electron in the

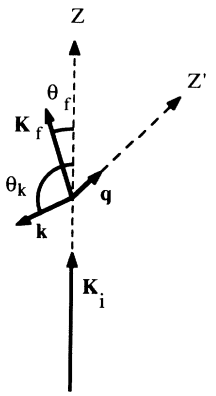

FIG. 1. Geometry of coplanar $(e,2e)$ reactions.

direction (θ_f,ϕ_f) into the solid angle $d\Omega_f$ is then given by

$$\frac{d^5\sigma}{d\Omega_f d\Omega_k d^3\mathbf{k}}=(2\pi)^4\frac{2K_f}{K_i}(\tfrac{1}{4}|T_{fi}^d+T_{fi}^{\rm ex}|^2 + \tfrac{3}{4}|T_{fi}^d-T_{fi}^{\rm ex}|^2) . \quad (43)$$

The matrix element T_{fi} can be written as

$$T_{fi}=\int d\mathbf{r}\psi_{\mathbf{K}_f}^{(-)*}(\mathbf{r})U_{1s\to\mathbf{k}}(\mathbf{r})\psi_{\mathbf{K}_i}^{(+)}(\mathbf{r}) \quad (44)$$

with

$$U_{1s\to\mathbf{k}}(\mathbf{r})=\int d\mathbf{r}'\psi_{\mathbf{k}}^{(-)*}(\mathbf{r}')\frac{1}{|\mathbf{r}-\mathbf{r}'|}\phi_{1s}(r') . \quad (45)$$

Using the integral representation of the confluent hypergeometric function [19]

$$ {}_1F_1(-c,1;-i(kr'+\mathbf{k}\cdot\mathbf{r}')) = \frac{1}{\Gamma(1-c)\Gamma(c)}\int_0^1 e^{i(kr'+\mathbf{k}\cdot\mathbf{r}')t}t^{c-1}(1-t)^{-c}dt , \quad (46)$$

where $c=iZ_T/k+\epsilon$, ϵ being an infinitesimal which will be set equal to zero after evaluating the integral, we may write the matrix element $U_{1s\to\mathbf{k}}$ as

$$U_{1s\to\mathbf{k}}(\mathbf{r})=\frac{N_k^{(-)*}}{\Gamma(1-c)\Gamma(c)}\left[\frac{Z_T^3}{\pi}\right]^{1/2} \times\int_0^1 dt\, t^{c-1}(1-t)^{-c} \times\int d^3r'\frac{e^{i(t-1)\mathbf{k}\cdot\mathbf{r}'-(Z_T-ikt)r'}}{|\mathbf{r}-\mathbf{r}'|} . \quad (47)$$

This integral is evaluated by Fourier transforming $(1/|\mathbf{r}-\mathbf{r}'|)$ and using Feynman integration to evaluate the integral over the momentum variables. We obtain

$$U_{1s\to\mathbf{k}}(\mathbf{r})=-4\pi\frac{N_k^{(-)*}}{\Gamma(1-c)\Gamma(c)}\left[\frac{Z_T^3}{\pi}\right]^{1/2} \times\int_0^1 dt\, t^{c-1}(1-t)^{-c}\frac{\partial}{\partial\mu} \times\int_0^1 dx\frac{1}{y}e^{i\mathbf{p}_1\cdot\mathbf{r}(1-x)-yr} , \quad (48)$$

where $\mu=Z_T-ikt$ and $\mathbf{p}_1=\mathbf{k}(t-1)$, and

$$y=[(1-x)(\mu^2+xp_1^2)]^{1/2} . \quad (49)$$

The matrix element $T_{\mathbf{k},1s}$ is then given by

$$T_{\mathbf{k},1s}=2\pi\frac{N_{K_i}^{(+)}N_{K_f}^{(-)*}N_k^{(-)*}}{\Gamma(1-c)\Gamma(c)}\left[\frac{Z_T^3}{\pi}\right]^{1/2} \times\int_0^1 dt\, t^{c-1}(1-t)^{-c}\frac{\partial}{\partial\mu}\int_0^1 dx\frac{1}{y}\int d^3r_1 F_1[a,1;i(K_ir-\mathbf{K}_i\cdot\mathbf{r})]\,{}_1F_1[b,1;i(K_fr+\mathbf{K}_f\cdot\mathbf{r})]\times e^{i(\mathbf{K}_i+\mathbf{K}_f-p\mathbf{k}_b)\cdot\mathbf{r}-yr}$$
$$=2\frac{N_{K_i}^{(+)}N_{K_f}^{(-)*}N_k^{(-)*}}{\Gamma(1-c)\Gamma(c)}\left[\frac{Z_T^3}{\pi}\right]^{1/2}\int_0^1 dt\, t^{c-1}(1-t)^{-c}\frac{\partial}{\partial\mu}\int_0^1 dx\frac{1}{y}\frac{\partial}{\partial y}I_{ab} , \quad (50)$$

where $p=(1-x)(1-t)$ and I_{ab} is defined by [20]

$$I_{ab}=\int d^3r_1 F_1[a,1;i(K_ir-\mathbf{K}_i\cdot\mathbf{r})]\,{}_1F_1(b,1;i(K_fr+\mathbf{K}_f\cdot\mathbf{r}))e^{i(\mathbf{K}_i-\mathbf{K}_f-p\mathbf{k})\cdot\mathbf{r}}\frac{e^{-yr}}{r} , \quad (51)$$

and given in Ref. [20] as a hypergeometric function

$$I_{ab}=\frac{4\pi C^{a+b-1}}{A^bB^a}\,{}_2F_1(a,b,1;z) , \quad (52)$$

where

$$\begin{aligned} A&=(y-ik)^2+(p\mathbf{k}-\mathbf{K}_i)^2 ,\\ B&=(y-iK_f)^2+(p\mathbf{k}+\mathbf{K}_f)^2 ,\\ C&=y^2+(p\mathbf{k}-\mathbf{K}_i+\mathbf{K}_f)^2 ,\\ D&=[y-i(K_i+K_f)]^2+p^2k^2 ,\\ z&=1-\frac{CD}{AB} . \end{aligned} \quad (53)$$

The matrix element $T_{\mathbf{k},1s}$ is then given by

$$T_{\mathbf{k},1s}=2\frac{N_{K_i}^{(+)}N_{K_f}^{(-)*}N_k^{(-)*}}{\Gamma(1-c)\Gamma(c)}\left[\frac{Z_T^3}{\pi}\right]^{1/2} \times\int_0^1 dt\, t^{c-1}(1-t)^{-c} \times\int_0^1 dx\left[-\frac{\mu(1-x)}{y^3}\frac{\partial I_{ab}}{\partial y}+\frac{1}{y}\frac{\partial^2 I_{ab}}{\partial y\partial\mu}\right] . \quad (54)$$

In order to evaluate the derivatives of I_{ab}, we write I_{ab} as

$$I_{ab}=4\pi\frac{C^{a+b-1}}{A^bB^a}\,{}_2F_1(a,b,1;z) =4\pi\frac{A^{a-1}B^{b-1}}{D^{a+b-1}}[(1-z)^{a+b-1}\,{}_2F_1(a,b;1;z)] \quad (55)$$

and

$$\frac{\partial I_{ab}}{\partial y}=\beta_y I_{ab}+\gamma_y I_{a,b+1}\ , \tag{56}$$

where

$$\beta=\left[(a-1)\frac{A'}{A}+(b-1)\frac{B'}{B}-(a+b-1)\frac{D'}{D}-\frac{b-(1-a)z}{1-z}\frac{z'}{z}\right], \tag{57}$$

$$\gamma=\frac{bD}{B(1-z)}\frac{z'}{z}\ , \tag{58}$$

and where the subscript indicates derivatives with respect to y. The derivatives with respect to μ are now easily evaluated as

$$\frac{\partial}{\partial\mu}\frac{\partial I_{ab}}{\partial y}=G_0 I_{ab}+G_1 I_{a,b+1}+G_2 I_{a,b+2}\ , \tag{59}$$

where

$$G_0=\alpha_y\left[\frac{\partial\beta_y}{\partial y}+\beta_y^2\right],$$

$$G_1=\alpha_y\left[\beta_y\gamma_y+\frac{\partial\gamma_y}{\partial y}+\gamma_y\beta_y^{b+1}\right], \tag{60}$$

$$G_2=\gamma_y\alpha_y\gamma_y^{b+1}\ ,$$

and

$$\alpha_y=\frac{\partial y}{\partial\mu}=\frac{(1-x)\mu}{y}\ , \tag{61}$$

and where the superscript $(b+1)$ indicates that γ and β are the coefficients of $I_{a,b+1}$ and $I_{a,b+2}$ in the expression for the derivative of $I_{a,b+1}$ [Eq. (56)].

The integral over x was evaluated numerically using a Gauss quadrature. The method of evaluation of the integral over t is presented in Appendix A.

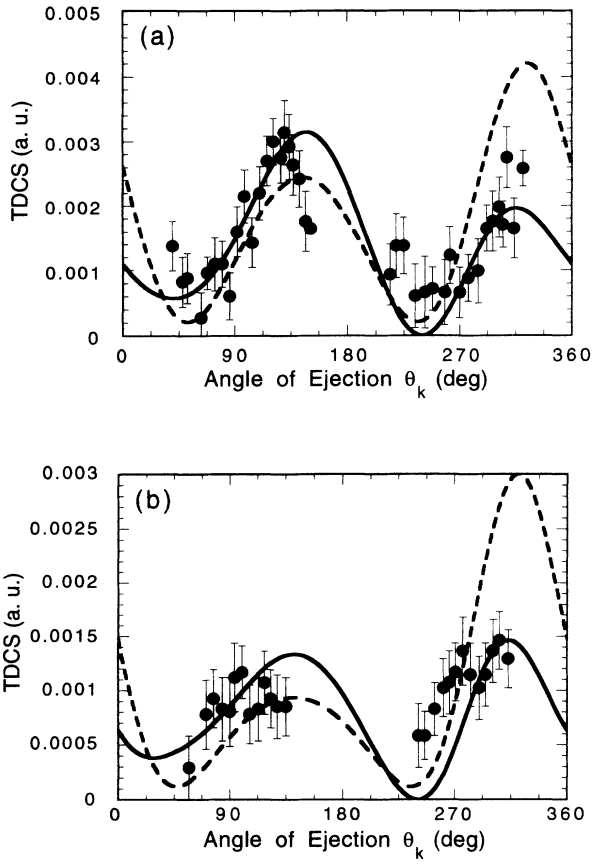

FIG. 2. Angular distribution of the TDCS for electron-impact ionization of carbon. Kinematical conditions: (a) $E_i=1801.2$ eV, $E_k=9.6$ eV, $\theta_f=4°$; (b) $E_i=1832.4$ eV, $E_k=41.0$ eV, $\theta_f=5°$. The solid line is the present calculation, the dashed line is a plane-wave Born calculation, and the solid dots are the experimental results from Ref. [9].

V. RESULTS AND DISCUSSION

A. Triple-differential cross section

Five different cases were studied and the results are shown in Figs. 2 and 3. The data shown in Fig. 2(a) correspond to an incident energy $E_i=1801.2$ eV, an energy of the ejected electron $E_k=9.6$ eV and a scattering angle $\theta_f=4°$, with a momentum transfer $|\mathbf{q}|=|\mathbf{K}_i-\mathbf{K}_f|=1.255$ a.u. The data shown in Fig. 2(b) correspond to $E_i=1832.04$ eV, $E_k=41$ eV, $\theta_f=5°$, and $q=1.457$ a.u. Solid lines correspond to the CBA, with $Z_{\rm eff}=Z_T$, and the dashed lines to the PBA case in which the TDCS is given in closed form [21]. The experimental results in Fig. 2 are from Ref. [9]; they are normalized to the present calculation. Notice that the main feature of the TDCS pointed out in Ref. [9], e.g., the presence of an intense recoil peak, which at $E_k=9.6$ eV is even larger than the binary one, is clearly reproduced in the CBA, while it is not reproduced in the PBA. We discuss this further in the next section based upon the occurrence of the different multipole components. The exact position of the peaks is not very well reproduced, but it should be pointed out that the experiment reported in Ref. [9] is on the $1s$ ionization of carbon in C_2H_2, while this theory uses a very simple model for both the $1s$ bound-state and final-state wave functions; specifically, the Coulomb phase shift of the wave function of the ejected electron might be different from the exact one, as well as the normalization. This was, in fact, noted in the second Born calculation of the TDCS for electron-impact ionization of helium of Mota Furtado and O'Mahony [5], where the wave function of the ejected electron was obtained from an R-matrix calculation, and the phase shifts for the $l\leq 3$ partial waves were found to be different from the Coulomb phases with $Z_{\rm eff}=Z_T$.

B. Multipole expansion of T_{fi}

In order to probe the validity of the Coulomb-Born dipole approximation, or the dipole approximation used in Ref. [9] to interpret the experimental results, and in order to analyze the results obtained in the CBA, we make a

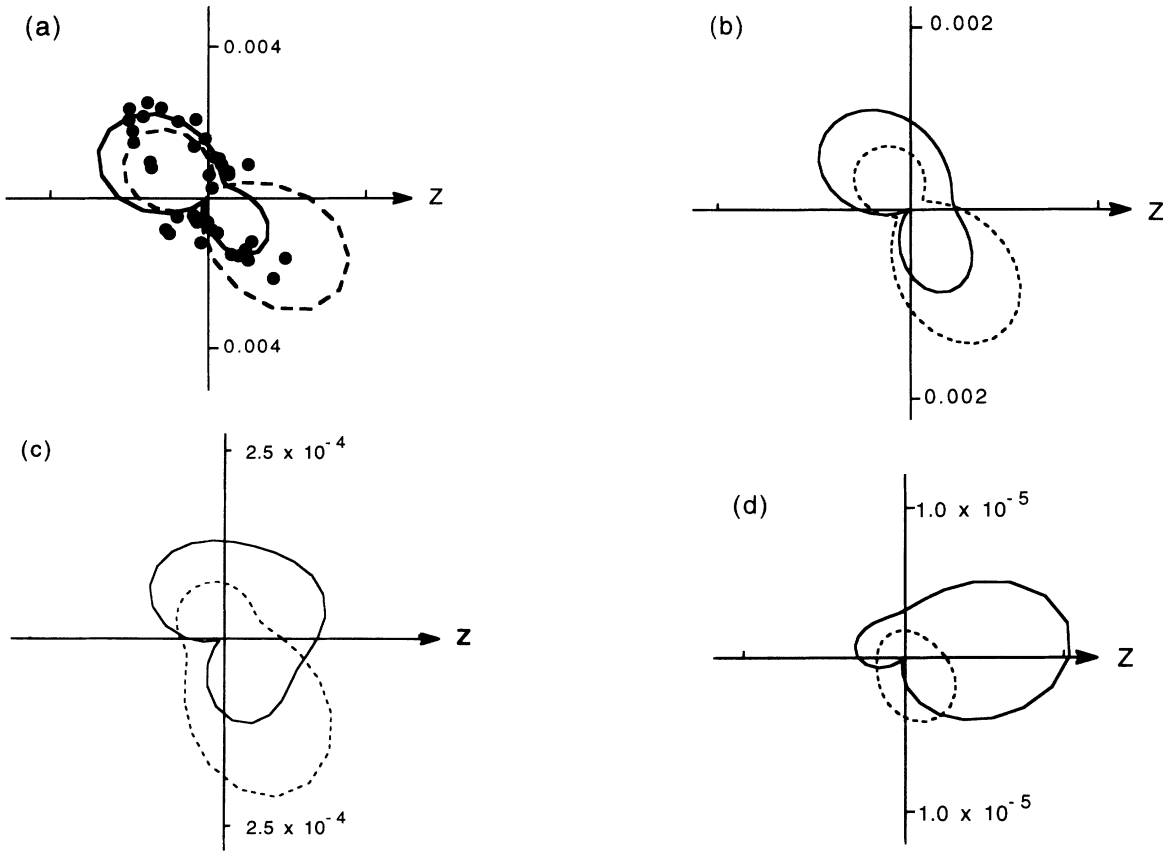

FIG. 3. Angular distribution of the TDCS for electron-impact ionization of carbon. Kinematical conditions: (a) $E_i=1801.2$ eV, $E_k=9.6$ eV, $\theta_f=4°$; (b) as (a) but $\theta_f=9°$, (c) as (a) but $\theta_f=20°$; and (d) as (a) but $\theta_f=40°$. The solid line is the present calculation, the dashed line is a plane-wave Born calculation, and the solid dots are the experimental results from Ref. [9].

multipole expansion of the T matrix relative to an axis parallel to the momentum transfer:

$$T_{fi}=\sum_{l,m} T_{l,m}\,Y_{lm}(\theta'_k,\phi'_k)\ , \tag{62}$$

where

$$T_{l,m}=\int T_{fi}\,Y_{lm}(\theta'_k,\phi'_k)\,d\Omega'_k \tag{63}$$

and compare with the PBA, in which case T_{lm} is given in closed form in Appendix C:

$$T_l^{PBA}=\frac{\sqrt{2\pi(2l+1)}N^{(-)*}Z^{5/2}}{\pi^3(Z-ik)^b q^2} \times\left[(b-1)f_l(b-2)-\frac{b+1}{Z-ik}f_l(b-1)\right], \tag{64}$$

TABLE I. Multiple components of the T matrix in CBA and PBA relative to an axis parallel to the momentum transfer. Kinematical conditions: $E_i=1801.2$ eV, $E_k=9.6$ eV, $\theta_f=4°$.

		CBA		PBA	
l	m	$\lvert T_{l,m}^{CBA}\rvert^2$	Phase	$\lvert T_l^{PBA}\rvert^2$	Phase
0	0	$0.351\,96\times10^{-3}$	135.0	$0.335\,6\times10^{-3}$	79.7
	1	$0.275\,33\times10^{-3}$	−89.5		
1	0	$0.118\,80\times10^{-1}$	0	$0.139\,72\times10^{-1}$	0
	2	$0.273\,70\times10^{-5}$	−163.3		
2	1	$0.136\,02\times10^{-5}$	68.0		
	0	$0.949\,77\times10^{-3}$	−91.8	$0.978\,17\times10^{-3}$	−69.9
	3	$0.319\,71\times10^{-7}$	−33.1		
	2	$0.613\,09\times10^{-6}$	136.5		
3	1	$0.116\,26\times10^{-5}$	42.0		
	0	0.19522×10^{-4}	−166.6	$0.195\,59\times10^{-4}$	−131.2

TABLE II. Multiple components of the T matrix in CBA and PBA relative to an axis parallel to the momentum transfer. Kinematical conditions: $E_i=1832.4$ eV, $E_k=41.0$ eV, $\theta_f=5°$.

		CBA		PBA	
l	m	$\lvert T_{l,m}^{\mathrm{CBA}}\rvert^2$	Phase	$\lvert T_l^{\mathrm{PBA}}\rvert^2$	Phase
0	0	$0.233\,31\times10^{-3}$	122.6	$0.213\,81\times10^{-3}$	69.3
	1	$0.168\,11\times10^{-3}$	−89.3		
1	0	$0.640\,63\times10^{-2}$	0	$0.730\,35\times10^{-2}$	0
	2	$0.297\,56\times10^{-5}$	−149.5		
2	1	$0.661\,48\times10^{-6}$	79.4		
	0	$0.735\,08\times10^{-3}$	−74.3	$0.761\,56\times10^{-3}$	−53.0
	3	$0.677\,54\times10^{-7}$	0		
	2	$0.106\,71\times10^{-5}$	169.2		
3	1	$0.135\,65\times10^{-5}$	−10.6		
	0	$0.274\,26\times10^{-4}$	−127.3	$0.289\,32\times10^{-4}$	−94.5

where

$$f_l(\gamma)=\frac{l!2^{l+1}}{(2l+1)!}\frac{\Gamma(1+\gamma)}{\Gamma(1+\gamma-l)}\times(-2kq)^l[Z^2+(q-k)^2]^{1+\gamma}\times{}_2F_1\left[-l,l-\gamma;2l+2;\frac{-4kq}{Z^2+(q-k)^2}\right]. \quad (65)$$

Table I gives the multipole components corresponding to $E_i=18\,001.2$ eV and Table II those corresponding to $E_i=1832.4$ eV. We see that, as expected, the $m=0$ dipole term is the dominant one both in CBA and PBA, and that for every l, the $m=0$ component is dominant. We also see three striking features: first, the absolute square of T_l is very similar in CBA and PBA, which means that generalized oscillator strengths in CBA are very much like those in PBA; second, that the phases relative to the $l=1$, $m=0$ component (given in the third and sixth columns) of the multipoles are very different in CBA and PBA, which means that the difference in the anisotropy of the ejected electrons in CBA and PBA is dictated mainly by the phases of the multipole components; and third, that there is a difference of nearly $\pi/2$ between the phases of the $m=1$ and the $m=0$ dipole components. This explains why the angular pattern of the TDCS is nearly aligned along the momentum-transfer axis, since, in a case in which all $T_{l\neq1,m}=0$, e.g., a purely dipole case, the angular distribution is along the momentum-transfer axis if the $m=0$ and 1 components have a relative phase of $\pi/2$. This $\pi/2$ phase difference is noted in Tables I and II. We show in Appendix C that this is an exact result in the CBA for peripheral collisions.

Another interesting feature of the angular distribution of the ejected electrons in CBA is the broadening of the waist compared to the PBA. This is also related to the relative phases of the multipole components, since it is clear that at an angle of $\theta_k'=\pi/2$ from the momentum-transfer vector there is a constructive interference between the (1,1) and the (2,0) components, which are almost in phase. The Y_{11} and Y_{20} have the same sign at that angle, while at an angle of $\theta_k'=-\pi/2$ the interference is destructive because now there is a factor of (-1) in Y_{11} coming from $e^{-im\phi_k'}$, since $\phi_k'=\pi$ in order to get values of $\theta<0$ in the collision plane. This feature is also predicted analytically for peripheral collisions in Appendix C, and was obtained in a distorted-wave calculation of electron-impact ionization of He at low energies [3]. This effect is enhanced at larger momentum transfers, as in Fig. 3, where we show polar plots of the TDCS for

TABLE III. Multiple components of the T matrix in CBA and PBA relative to an axis parallel to the momentum transfer. Kinematical conditions: $E_i=1801.2$ eV, $E_k=9.6$ eV, $\theta_f=9°$.

		CBA		PBA	
l	m	$\lvert T_{l,m}^{\mathrm{CBA}}\rvert^2$	Phase	$\lvert T_l^{\mathrm{PBA}}\rvert^2$	Phase
0	0	$0.309\,62\times10^{-3}$	118.5	$0.312\,18\times10^{-3}$	79.7
	1	$0.201\,83\times10^{-3}$	−88		
1	0	$0.499\,74\times10^{-2}$	0	$0.516\,52\times10^{-2}$	0
	2	$0.734\,81\times10^{-5}$	−170.8		
2	1	$0.445\,52\times10^{-6}$	170.7		
	0	$0.676\,55\times10^{-3}$	−88.8	$0.703\,96\times10^{-3}$	−69.9
	3	$0.165\,26\times10^{-6}$	−43.2		
	2	$0.110\,30\times10^{-5}$	122.7		
3	1	$0.295\,53\times10^{-7}$	−73.2		
	0	0.25925×10^{-4}	−157.6	$0.285\,69\times10^{-4}$	−131.2

TABLE IV. Multiple components of the T matrix in CBA and PBA relative to an axis parallel to the momentum transfer. Kinematical conditions: $E_i=1801.2$ eV, $E_k=9.6$ eV, $\theta_f=20°$.

		CBA		PBA	
l	m	$\lvert T_{l,m}^{\mathrm{CBA}}\rvert^2$	Phase	$\lvert T_l^{\mathrm{PBA}}\rvert^2$	Phase
0	0	$0.150\,09\times10^{-3}$	99.1	$0.167\,12\times10^{-3}$	79.7
	1	$0.371\,36\times10^{-3}$	−88.1		
1	0	$0.683\,41\times10^{-3}$	0	$0.703\,85\times10^{-3}$	0
	2	$0.303\,98\times10^{-5}$	−175.8		
2	1	$0.741\,19\times10^{-6}$	−152.3		
	0	$0.134\,01\times10^{-3}$	−87.1	$0.145\,92\times10^{-3}$	−69.9
	3	$0.736\,54\times10^{-7}$	−48.9		
	2	$0.300\,49\times10^{-6}$	113.7		
3	1	$0.876\,32\times10^{-7}$	134.0		
	0	$0.922\,19\times10^{-5}$	−159.2	$0.102\,18\times10^{-4}$	−131.2

$E_i=1801.2$ eV, and $E_k=9.6$ eV, $\theta_f=4°$ in (a), $\theta_f=9°$ in (b), $\theta_f=20°$ in (c) and $\theta_f=40°$ in (d). Multipole components for the last three cases are given in Tables III–V respectively. Notice that the similarity of the amplitudes of these components between the CBA and PBA is still present at 9° and 20°, while at 40° the difference between them has increased, especially because in CBA the monopole component is greater than the dipole. This also happens in the PBA [22] but at a larger momentum transfer. The relative phase of the dipole components at 40° is no longer $\pi/2$, and the angular distribution is not symmetric around the momentum-transfer axis.

VI. SUMMARY AND CONCLUSIONS

We have presented the results of a calculation of the TDCS for electron-impact ionization of inner shells of carbon using a perturbation theory that allows the use of Coulomb waves with arbitrary effective charge for the incoming and scattered electrons, thus extending the use of the CBA to scattering from neutral atoms, and have showed that the CBA reproduces most of the structural parameters of the TDCS, especially the ratio between the binary and recoil peaks. The position of the peaks is not very well reproduced, possibly due to the simplicity of the final-state wave function of the ejected electron. A more elaborate wave function, or an R-matrix treatment of this electron's wave function is needed to investigate this point.

A multipole expansion of the T matrix shows that, in the range of energies where the experiments were done, the contribution to the TDCS of the quadrupole term is appreciable and must be taken into account. This means that a dipole approximation is not valid in this energy range. We also see that the absolute square of the multipole amplitudes in CBA and PBA differ very little. This means that, even though the angular distribution of the ejected electrons is quite different in PBA and CBA, the generalized oscillator strengths are similar. This is an important feature of the generalized oscillator strengths, which should be investigated further. The phase [relative to the (1,0) component] of the multipole components are quite different in CBA and PBA. The main difference between the angular distribution of the TDCS in CBA and PBA is therefore due to the differing interference between the multipole components. We note that there is a difference of nearly $\pi/2$ in the phases of the two dipole terms, which give by far the dominant contribution. This means that the angular pattern of the TDCS should be nearly aligned along the momentum-transfer axis. This

TABLE V. Multiple components of the T matrix in CBA and PBA relative to an axis parallel to the momentum transfer. Kinematical conditions: $E_i=1801.2$ eV, $E_k=9.6$ eV, $\theta_f=40°$.

		CBA		PBA	
l	m	$\lvert T_{l,m}^{\mathrm{CBA}}\rvert^2$	Phase	$\lvert T_l^{\mathrm{PBA}}\rvert^2$	Phase
0	0	$0.180\,07\times10^{-4}$	85.8	$0.126\,85\times10^{-4}$	79.7
	1	$0.357\,36\times10^{-5}$	−123.5		
1	0	$0.164\,37\times10^{-4}$	0	$0.144\,49\times10^{-4}$	0
	2	$0.346\,17\times10^{-6}$	−121.0		
2	1	$0.143\,72\times10^{-6}$	−149.1		
	0	$0.192\,54\times10^{-4}$	−81.5	$0.1189\,56\times10^{-5}$	−69.9
	3	$0.968\,07\times10^{-8}$	−91.9		
	2	$0.164\,20\times10^{-7}$	101.5		
3	1	$0.695\,52\times10^{-8}$	108.0		
	0	$0.681\,30\times10^{-7}$	−152.4	$0.964\,55\times10^{-9}$	−131.2

approximate symmetry of the TDCS along the momentum transfer is not present at larger momentum transfers, where the monopole contribution increases, and the interference pattern between the different multipole components becomes more complicated.

ACKNOWLEDGMENTS

Discussions with S. J. Ward and M. Brauner are gratefully acknowledged. One of us (J.B.) thanks the Escuela Colombiana de Ingeniería for granting him a leave of absence and for their unconditional support for many years. This research has been sponsored by the U.S. Department of Energy under Contract No. DE-ACOS-840OR21400 with Martin Marietta Energy Systems, Inc.

APPENDIX A: EVALUATION OF AN INTEGRAL

It is well known that the numerical evaluation of integrals of the form of

$$I=\int_0^1 dt\, t^{c-1+\epsilon}(1-t)^{-c}F(t) \tag{A1}$$

is very difficult when c is large and complex, due to fast oscillations at the end points. In order to overcome this difficulty we expand $F(t)$ in a basis of Legendre polynomials and integrate the fast oscillatory part of the integrand analytically:

$$F(t)=\sum_{l=0}^{l_{\max}} a_l P_l(1-2t)\ , \tag{A2}$$

where a_l is given by

$$a_l=(2l+1)\int_0^1 F(t)P_l(1-2t)dt\ . \tag{A3}$$

We use a power-series expansion for P_l and substitute Eq. (A3) into Eq. (A1) to obtain

$$I=\sum_{l=0}^{l_{\max}} a_l \sum_{n=0}^{l}\frac{(-l)_n(l+1)_n}{n!n!}\times\int_0^1 dt\, t^{c+n-1+n}(1-t)^{-c}\ . \tag{A4}$$

The integral over t can now be evaluated exactly to obtain (taking the limit $\epsilon\to 0$)

$$I=\sum_{l=0}^{l_{\max}} a_l \sum_{n=0}^{l}\frac{(-l)_n(l+1)_n}{n!n!}\frac{\Gamma(c+n)\Gamma(1-c)}{\Gamma(n+1)}\ . \tag{A5}$$

APPENDIX B: MULTIPOLE COMPONENTS OF THE T MATRIX IN PBA

The transition matrix element in the PBA is given by

$$T_{fi}^{PBA}=\left\langle \Phi_{\mathbf{K}_f}(\mathbf{r})\psi_{\mathbf{k}}^{(-)}(\mathbf{r}')\left|\frac{1}{|\mathbf{r}-\mathbf{r}'|}\right|\phi_i(\mathbf{r}')\Phi_{\mathbf{K}_i}(r)\right\rangle$$
$$=\frac{1}{(2\pi)^3}\frac{4\pi}{q^2}\langle\psi_{\mathbf{k}}^{(-)}|e^{i\mathbf{q}\cdot\mathbf{r}}|\phi_i(\mathbf{r})\rangle\ , \tag{B1}$$

where $\mathbf{q}=\mathbf{K}_i-\mathbf{K}_f$ is the momentum transfer of the electron. We may then write T_{fi}^{PBA} using the function I_{ab} of Eqs. (51)–(53):

$$T_{fi}^{\mathrm{PBA}}=\frac{1}{(2\pi)^3}\frac{4\pi}{q^2}N^{-*}(2\pi)^{3/2}\frac{2Z^{3/2}}{\sqrt{4\pi}}\frac{\partial}{\partial x}I_{a=0,b}(x)\Big|_{x=Z}\ , \tag{B2}$$

where now A and C in I_{ab} are given by

$$\begin{aligned} C&=x^2+(\mathbf{q}-\mathbf{k})^2\ ,\\ A&=(x-ik)^2+q^2\ . \end{aligned} \tag{B3}$$

The l component of the T matrix is therefore given by

$$T_l^{\mathrm{PBA}}=\left[\frac{2l+l}{4\pi}\right]^{1/2}2\pi\int T_{fi}^{\mathrm{PBA}}P_l(\cos\theta)d(\cos\theta)$$
$$=\frac{\sqrt{2\pi(2l+1)}N^{-*}Z^{5/2}}{\pi^3(Z-ik)^b q^2}\left[(b-1)f_l(b-2)-\frac{b+1}{Z-ik}f_l(b-1)\right]\ , \tag{B4}$$

where

$$f_l(\gamma)=\int_{-1}^{1}(Z^2+q^2+k^2-2kq\cos\theta)^{\gamma}P_l(\cos\theta)d(\cos\theta)$$
$$=\frac{l!2^{l+1}}{(2l+1)!}\frac{\Gamma(1+\gamma)}{\Gamma(1+\gamma-l)}(-2kq)^l[Z^2+(q-k)^2]^{1+\gamma}{}_2F_1\left[-l,l-\gamma;2l+2;\frac{-4kq}{Z^2+(q-k)^2}\right]\ , \tag{B5}$$

and where we have used Rodriquez's formula and integrated by parts l times in order to do the integral over the Legendre polynomials.

APPENDIX C: RELATIVE PHASE OF THE DIPOLE TERMS IN PERIPHERAL COLLISIONS

Peripheral collisions occur when the incident electron penetrates only the outer layer of the electron charge cloud. Since monopole transitions require that the incident electron penetrate deeply into the electron cloud, a dipole approximation is appropriate in these cases. The transition matrix is then

$$T_{\mathbf{kp},1s}=\langle \psi^{+}_{\mathbf{K}_i}(\mathbf{r})|U_{1s\to\mathbf{kp}}(\mathbf{r})|\psi^{-}_{\mathbf{K}_f}(\mathbf{r})\rangle \ , \tag{C1}$$

where $U_{1s\to\mathbf{k}p}(\mathbf{r})$ is given by

$$U_{1s\to\mathbf{k}p}(r)=\mathcal{N}\int_0^1 dt\, t^{1+c}(1-t)^{1-c}\left[\frac{2}{x^3}-\frac{1}{x^2}\frac{\partial}{\partial x}\mathbf{I}\right] , \tag{C2}$$

$\mathcal{N}$ is a normalization constant and $\mathbf{I}$ is given by

$$\begin{aligned}\mathbf{I}&=\left\langle \psi^{+}_{\mathbf{K}_i}(\mathbf{r})\left|\frac{\mathbf{r}}{r^3}\right|\psi^{-}_{\mathbf{K}_f}(\mathbf{r})\right\rangle \\ &=-\frac{1}{Z-1}\langle \psi^{+}_{\mathbf{K}_i}(\mathbf{r})|[H,\nabla]|\psi^{-}_{\mathbf{K}_f}(\mathbf{r})\rangle \ ,\end{aligned} \tag{C3}$$

where we have used the commutator relation

$$\frac{\mathbf{r}'}{r'^3}=-\frac{1}{Z-1}[H,\nabla] \ . \tag{C4}$$

The magnetic substates are now given as the components of the vector $\mathbf{I}$. Using the results from Ref. [20] we obtain.

$$\begin{aligned}\mathbf{I}\cdot\mathbf{q}=&4\pi i\left[\frac{q^2}{q_\parallel}\right]^{-(a+b)}(K_i+K_f)^{(a+b)} \\ &\times e^{i\pi(a-b)/2}\Gamma(1+a)\Gamma(1+b)\tfrac{1}{2} \\ &\times\left[{}_2F_1\left[a,b+1;1;-\frac{q_\perp^2}{q_\parallel^2}\right]\right. \\ &\left.+{}_2F_1\left[a+1,b;1;-\frac{q_\perp^2}{q_\parallel^2}\right]\right] ,\end{aligned} \tag{C5}$$

where $\mathbf{q}=\mathbf{K}_i-\mathbf{K}_f$ is the momentum transfer and $q_\perp$ and $q_\parallel$ are its components perpendicular and parallel to K_i, respectively. We now compute the complex conjugate of Eq. (C5) as

$$\begin{aligned}\mathbf{I}^*\cdot\mathbf{q}=&\left[4\pi i\left[\frac{q^2}{q_\parallel}\right]^{a+b}(K_i+K_f)^{-(a+b)}e^{i\pi(a-b)/2}\Gamma(1-a)\Gamma(1-b)\frac{1}{2}\right]^* \\ &\times\left[{}_2F_1\left[-a,-b+1;1;-\frac{q_\perp^2}{q_\parallel^2}\right]+{}_2F_1\left[-a+1,-b;1;-\frac{q_\perp^2}{q_\parallel^2}\right]\right] \\ =&e^{i\Phi}\mathbf{I}\cdot\mathbf{q} \ ,\end{aligned} \tag{C6}$$

where we have used Eq. (15.3.3) of Ref. [19], and where $e^{i\Phi}$ is given by

$$e^{i\Phi}=\left[\frac{q^2}{q_\parallel}\right]^{-2(a+b)}\frac{\Gamma(1+a)\Gamma(1+b)}{\Gamma(1-a)\Gamma(1-b)}(K_i+K_f)^{2(a+b)}\left[1+\frac{q_\perp^2}{q_\parallel^2}\right]^{a+b} . \tag{C7}$$

We now define a vector $\mathbf{q}_1=(\mathbf{K}_i+\mathbf{K}_f)/(K_i+K_f)$ and form a vector perpendicular to $\mathbf{q}$ as $\mathbf{q}_2=(\mathbf{q}\times\mathbf{q}_1)\times\mathbf{q}$. We then have

$$\mathbf{I}\cdot\mathbf{q}_2/q^2=\mathbf{I}\cdot\mathbf{q}_1-\mathbf{I}\cdot\mathbf{q}\frac{q_\parallel}{q^2} \ , \tag{C8}$$

where

$$\begin{aligned}\mathbf{I}\cdot\mathbf{q}_1=&4\pi i\left[\frac{q^2}{q_\parallel}\right]^{a+b}(K_i+K_f)^{-(a+b)}e^{i\pi(a-b)/2}\Gamma(1-a)\Gamma(1-b) \\ &\times\left\{\frac{q_\parallel}{q^2}{}_2F_1\left[a,b;1;-\frac{q_\perp^2}{q_\parallel^2}\right]+\left[\frac{1}{2(k+k')}\right]\left[{}_2F_1\left[a,b+1;1;-\frac{q_\perp^2}{q_\parallel^2}\right]-{}_2F_1\left[a+1,b;1;-\frac{q_\perp^2}{q_\parallel^2}\right]\right]\right\} .\end{aligned} \tag{C9}$$

Using Eq. (15.2.14) of Ref. [19] we can write Eq. (C8) as

$$\mathbf{I}\cdot\mathbf{q}_2/q^2=\left[4\pi i\left[\frac{q^2}{q_\parallel}\right]^{a+b}(K_i+K_f)^{-(a+b)}e^{i\pi(a-b)/2}\Gamma(1-a)\Gamma(1-b)\right]\left[-\frac{q_\parallel}{q^2}\frac{a+b}{a-b}+\frac{1}{2(K_i+K_f)}\right]$$
$$\times\left[{}_2F_1\left[-a,-b+1;1;-\frac{q_\perp^2}{q_\parallel^2}\right]-{}_2F_1\left[-a+1,-b;1;-\frac{q_\perp^2}{q_\parallel^2}\right]\right]. \tag{C10}$$

We now compute the complex conjugate of Eq. (C8) and use Eq. (15.3.3) of Ref. [19] to obtain

$$\mathbf{I}^*\cdot\mathbf{q}_2/q^2=-e^{i\Phi}\mathbf{I}\cdot\mathbf{q}_2/q^2\ . \tag{C11}$$

This shows that the component of **I** along **q** is 90° out of phase relative to the component along a vector perpendicular to **q** and in the scattering plane. Since the components of **I** give the magnetic substates of T_{fi}, this shows that the dipole pattern remains aligned along q just as in the normal Born approximation but is broadened at the waist, and this broadening represents an orientation of the final state.

---

*On leave from Escuela Colombiana de Ingeniería, Bogotá, Colombia.

[1] H. Ehrhardt, K. Jung, G. Knoth, and P. Schlemmer, Z. Phys. D **1**, 3 (1986), and references therein.
[2] F. W. Byron, Jr. and C. J. Joachain, Phys. Rep. **179**, 213 (1989).
[3] D. H. Madison, R. V. Calhoun, and W. N. Shelton, Phys. Rev. A **16**, 552 (1977).
[4] X. Zhang, C. T. Whelan, and H. R. Walters, J. Phys. B **23**, L173 (1990).
[5] F. Mota Furtado and P. F. O'Mahony, J. Phys. B **20**, L405 (1988).
[6] M. Brauner, J. S. Briggs, and J. T. Broad, J. Phys. B **24**, 287 (1991).
[7] A. Franz and H. Klar, Z. Phys. D **1**, 572 (1986).
[8] J. Botero and J. H. Macek, J. Phys. B **24**, L405 (1991).
[9] L. Avaldi, R. Camilloni, and G. Stefani, Phys. Rev. A **41**, 134 (1990).
[10] P. Bickert and W. Hink (unpublished).
[11] A. Lahman-Bennani, H. F. Wellenstaein, A. Duguet, and A. Daoud, J. Phys. B **30**, 1511 (1984).
[12] G. Stefani, L. Avaldi, A. Lahmam-Bennani, and A. Duguet, J. Phys. B **19**, 3787 (1986).
[13] R. Mapleton, Proc. R. Soc. **91**, 868 (1967).
[14] M. R. H. Rudge, J. Phys. **2**, L130 (1968).
[15] R. G. Newton, *Scattering Theory of Waves and Particles* (Springer-Verlag, New York, 1982), p. 426.
[16] J. Macek, Phys. Rev. A **37**, 2365 (1988).
[17] M. J. Roberts, J. Phys. B **18**, L707 (1985).
[18] B. H. Bransden and J. P. Dewangen in *Advances in Atomic and Molecular Physics,* edited by D. Bates and B. Bederson (Academic, London, 1988), Vol. 25, p. 343.
[19] *Handbood of Mathematical Functions,* edited by M. Abramowitz and I. A. Stegun (Dover, New York, 1965), p. 505.
[20] Sung Dahm Oh, J. H. Macek, and E. Kelsey, Phys. Rev. A **17**, 873 (1978).
[21] N. F. Mott and H. S. W. Massey, *The Theory of Atomic Collisions* (Oxford University, London, 1965), p. 489.
[22] M. Inokuti, Rev. Mod. Phys. **43**, 297 (1971); M. Inokuti, Y. Itikawa, and J. M. Turner, *ibid.* **50**, 23 (1978).